Identification of a dynamical model of a thermally actuated deformable mirror

Aleksandar Haber,[1,*] Alessandro Polo,[2] Simon Ravensbergen,[3] H. Paul Urbach,[2] and Michel Verhaegen[1]

[1]*Delft Center for Systems and Control, Delft University of Technology, 2628 CD Delft, The Netherlands*

[2]*Optics Research Group, Delft University of Technology, Lorentzweg 1, 2628 CJ Delft, The Netherlands*

[3]*Technische Universiteit Eindhoven, Den Dolech 2, 5612 AZ Eindhoven, The Netherlands*

**Corresponding author: a.haber@tudelft.nl*

Received June 25, 2013; revised July 8, 2013; accepted July 8, 2013;
posted July 9, 2013 (Doc. ID 192778); published August 8, 2013

Using the subspace identification technique, we identify a finite dimensional, dynamical model of a recently developed prototype of a thermally actuated deformable mirror (TADM). The main advantage of the identified model over the models described by partial differential equations is its low complexity and low dimensionality. Consequently, the identified model can be easily used for high-performance feedback or feed-forward control. The experimental results show good agreement between the dynamical response predicted by the model and the measured response of the TADM. © 2013 Optical Society of America

OCIS codes: (010.1080) Active or adaptive optics; (220.1000) Aberration compensation; (230.4040) Mirrors.
http://dx.doi.org/10.1364/OL.38.003061

In a large variety of adaptive optics (AO) applications [1–7], slowly varying or static wavefront aberrations must be corrected accurately. Thermally actuated deformable mirrors (TADMs) are suitable for these AO applications because they have a high position resolution with high reproducibility [8]. Furthermore, they are less expensive than other types of deformable mirrors (DMs), like membrane or piezoelectric DMs [6,7].

In [4], a TADM has been used to correct static wavefront aberrations. In the above cited paper, a static (steady-state) model of the TADM has been identified and, on the basis of this model, a control action for the TADM has been derived as the solution of a constrained least-squares problem. However, this control strategy requires that the time between two consecutive control iterations is approximately equal to the settling time (or the rise time) of the TADM. Consequently, this wavefront correction strategy is relatively slow and its performance might be additionally degraded in the case of time-varying wavefront aberrations.

To achieve fast correction of both static and time-varying wavefront aberrations, the time between control iterations has to be significantly smaller than the TADM's settling time. In such cases, a dynamical model of a TADM has to be developed to accurately correct wavefront aberrations [9,10]. Once this dynamical model has been obtained, model-based control strategies [11,12] can be employed to maximize the performance of the wavefront correction. Apart from the control perspective, a dynamical model of a TADM is important because it can be used to simulate the dynamical behavior of the AO system before the real system has been built.

A dynamical model of a TADM must meet two requirements. First, it must accurately capture the TADM's dynamics. Second, to be used for control, it must be relatively simple [13,14] and preferably low dimensional (i.e., it must have a relatively small number of states). However, the dynamics of TADMs are governed by the thermoelastic system of partial differential equations (PDEs) [15]. Furthermore, in the case of the TADMs that have been proposed in [3,7], the thermoelastic system of PDEs must be coupled with the biharmonic plate equation [16]. The dynamical model based on these PDEs is infinite-dimensional and as such is too complex to be used for control. To apply the model-based control strategies of [11,12], a more compact, finite-dimensional model must be developed. One way to develop such a model would be to discretize the system of PDEs and corresponding boundary conditions using the finite element method (FEM) [17]. However, the FEM can be applied only if all physical parameters of the TADM are known. Furthermore, the FEM model is usually high dimensional and thus is still relatively complex to be used for control.

In this Letter, we follow another way of model building that is based on system identification techniques [18]. Accordingly, from experimental data, we identify a low-order, state-space model of a recently developed TADM prototype. This device has been developed by Eindhoven University of Technology [3,8]. We have identified the dynamical model of the TADM using the subspace identification technique [18,19]. Due to its low dimensionality, the identified model can be easily used to design feed-forward or feed-back model-based controllers. As we will show later, the experimental results show a good match between the identified state-space model and the response of the TADM.

Figure 1 shows the TADM sketch. The mirror B and the backplate A, are connected with 19 thermomechanical actuators C. The mirror diameter is 30 mm and the

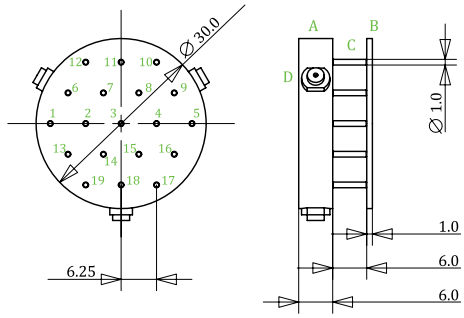


Fig. 1. Sketch of the thermally actuated DM.

 © 2013 Optical Society of America

19 actuators are placed inside of a circle with a diameter of 25 mm. The actuators consist of aluminum rods with heating coils warped around them. When voltage is applied to an actuator it heats up and elongates. As it elongates, it exerts a mechanical force that deforms the mirror and a supporting back plate A. To identify the model of the TADM, we built an experimental setup where the surface of the TADM is illuminated by coherent light coming from a semiconductor laser of wavelength $\lambda = 638$ nm. The wavefront reflected by TADM is measured by a Shack–Hartmann Wavefront Sensor (S-H WFS) (Thorlabs WFS S300-14AR, 1.3 Mpixel, $\lambda/50$ rms accuracy). The mirror and the S-H WFS optically conjugate through a relay system consisting of two spherical lenses.

In general, the sampling period should be 5–10 times shorter than the rise time of the TADM [18]. Our experimental results show that the TADM rise time is approximately 15 s, which is in agreement with the results reported in [3]. Consequently, we chose a control and measurement sampling period of 2 s [18]. In this Letter, k will denote a discrete time instant corresponding to this sampling period. The wavefront produced by the TADM, at the time instant k, and that is sensed by the S-H WFS, is represented using a Zernike polynomial expansion (Noll [20]): $\Phi(x,y,k) = \sum_{i=1}^{36} \alpha_i(k) Z_i(x,y)$, where $\Phi(x,y,k)$ is the spatial distribution of the wavefront, $\alpha_i(k)$ is the ith coefficient of the Zernike polynomial expansion, and $Z_i(x,y)$ is the ith Zernike polynomial. All static wavefront aberrations that originate from the initial nonflatness of the TADM and from imperfections and misalignments of the optical components in the system, are subtracted from the measured wavefront.

The model of the TADM was identified using the following procedure [18]. First, we determined which Zernike coefficients were excited when we randomly actuated the TADM. It helped us to define the outputs of the model. Next, we investigated the TADM's linearity. On the basis of this analysis, we postulated a state-space model of the TADM. In the final step, we identified the state-space model and assessed its quality.

To constrain the outputs of the model, we randomly actuated all 19 actuators over a time period of two minutes and recorded the amplitudes of all 36 measured Zernike coefficients. By analyzing this measurement data, we concluded that during the random actuation of the TADM, the first 10 Zernike coefficients were excited while others did not show a significant contribution to the measured wavefront. Therefore, the output of the model should consist of the first 10 Zernike coefficients: $\mathbf{y}(k) = [\alpha_2(k)\ \alpha_3(k)\ \ldots\ \alpha_{10}(k)]^T$ (where we neglect the first coefficient; i.e., piston). The voltage applied to the ith actuator (input of the model) will be denoted by v_i (expressed as between 0% and 100% of the maximum voltage).

To analyze the step response, we applied the step functions of different magnitudes to the actuators and measured each response. Figure 2 shows the measured responses of the third actuator.

Figure 2(b) shows that the steady-state deformation of the TADM is a quadratic function of inputs. This is an experimental confirmation that the heat generated at the actuator is a quadratic function of the applied

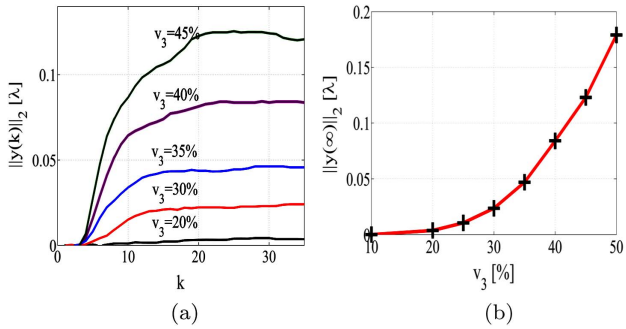


Fig. 2. Step response of the TADM when the step functions are applied to the third actuator: (a) the RMS $\|\mathbf{y}(k)\|_2$. (b) Steady-state value of the RMS $\|\mathbf{y}(\infty)\|_2$.

voltages [3]. As we show later, this nonlinearity can be eliminated from the model by defining new inputs that are squares of the voltages applied to the actuators.

Next, we tested the superposition principle between several actuators. Figure 3 shows the results of the superposition test between actuators 2 and 4. We applied a 40% voltage step to actuator 2 and measured the response (v_2 in Fig. 3). Next, we applied a 40% voltage step to actuator 4 and measured the response. Finally, we actuated actuators 2 and 4 together ($\mathrm{v}_2\&\mathrm{v}_4$ in Fig. 3) and measured the response.

The experimental results shown in Figs. 2 and 3 indicate that the TADM can be modeled as a linear state-space model where the inputs are squares of the voltages:

$$\mathbf{x}(k+1) = A\mathbf{x}(k) + B\mathbf{u}(k) \tag{1}$$

and

$$\mathbf{y}(k) = C\mathbf{x}(k) + \mathbf{e}(k), \tag{2}$$

where $\mathbf{x}(k) \in \mathbb{R}^n$ is the state, n is the system order, $\mathbf{u}(k) = [(\mathrm{v}_1(k))^2\ (\mathrm{v}_2(k))^2\ \ldots\ (\mathrm{v}_{19}(k))^2]$ is the input vector of the squared voltages, $A \in \mathbb{R}^{n\times n}$, $B \in \mathbb{R}^{n\times 19}$ and $C \in \mathbb{R}^{9\times n}$ are the system matrices and $\mathbf{e}(k) \in \mathbb{R}^9$ is a S-H WFS measurement noise.

The identification problem of the state-space model (1) and (2), can be formulated as follows. From the sequence of the input–output data: $\{\mathbf{y}(k), \mathbf{u}(k)\}$, $k = 0, 1, \ldots, N$, estimate the system order n and the system matrices A, and C of the state-space model (1) and (2). The length N of the data sequence $\{\mathbf{y}(k), \mathbf{u}(k)\}$ should be chosen so the total measurement time is at least 10 times longer than

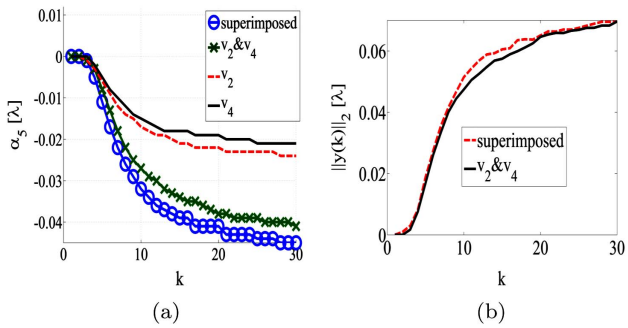


Fig. 3. Test of the superposition principle: (a) 5th Zernike coefficient and (b) the RMS of the total measured wavefront.

the time constant (or roughly the rise time) of the TADM [18]. In general, the larger the length of the data sequence, the better the quality of the identified model. We chose $N = 450$. The estimates of A, B, and C will be denoted by $\hat{A}$, $\hat{B}$ and $\hat{C}$, respectively. To identify the state-space model we used the predictor-based subspace identification method [10,19]. Similar identification results can be obtained using other subspace identification techniques [18].

We use the following strategy to assess the quality of the identified model. First, we generated an input sequence that is different from the input sequence that has been used for identification. Let such an input sequence be denoted by $\{\mathbf{u}_2(k)\}$. Then, using this input we actuated the TADM and generated the output data sequence $\{\mathbf{y}_2(k)\}$. From this input–output data, we estimate the initial state of (1) and (2) using the following methodology. By substituting the system matrices with their estimates, from (1) and (2) we obtain:

$$\underline{\mathbf{y}}_2 = \hat{O}\mathbf{x}(0) + \hat{D}\underline{\mathbf{u}}_2 + \underline{\mathbf{e}}_2, \tag{3}$$

where

$$\underline{\mathbf{y}}_2 = \begin{bmatrix} \mathbf{y}_2(0) \\ \mathbf{y}_2(1) \\ \vdots \\ \mathbf{y}_2(M) \end{bmatrix}, \quad \underline{\mathbf{u}}_2 = \begin{bmatrix} \mathbf{u}_2(0) \\ \mathbf{u}_2(1) \\ \vdots \\ \mathbf{u}_2(M) \end{bmatrix},$$

$$\underline{\mathbf{e}}_2 = \begin{bmatrix} \mathbf{e}_2(0) \\ \mathbf{e}_2(1) \\ \vdots \\ \mathbf{e}_2(M) \end{bmatrix}, \quad \hat{O} = \begin{bmatrix} \hat{C} \\ \hat{C}\hat{A} \\ \vdots \\ \hat{C}\hat{A}^M \end{bmatrix},$$

$$\hat{D} = \begin{bmatrix} 0 & 0 & 0 & \dots & 0 \\ \hat{C}\hat{B} & 0 & 0 & \dots & 0 \\ \hat{C}\hat{A}\hat{B} & \hat{C}\hat{B} & 0 & \dots & 0 \\ \vdots & & \ddots & \ddots & \\ \hat{C}\hat{A}^{M-1}\hat{B} & \hat{C}\hat{A}^{M-2}\hat{B} & & \hat{C}\hat{B} & 0 \end{bmatrix} \tag{4}$$

and where M should be chosen such that $\hat{O}$ has full column rank. The initial state $\mathbf{x}(0)$ is estimated by solving the following least-squares problem:

$$\min_{\mathbf{x}(0)} \|\underline{\mathbf{z}} - \hat{O}\mathbf{x}(0)\|_2^2, \tag{5}$$

where $\underline{\mathbf{z}} = \underline{\mathbf{y}}_2 - \hat{D}\underline{\mathbf{u}}_2$. The solution of (5) is $\hat{\mathbf{x}}(0) = \hat{O}^{\dagger}\underline{\mathbf{z}}$, where $\hat{O}^{\dagger} = (\hat{O}^T\hat{O})^{-1}\hat{O}^T$ denotes the matrix pseudo-inverse. Starting from $\hat{\mathbf{x}}(0)$ and using $\{\mathbf{u}_2(k)\}$, we simulate the identified version of the state–space model (1) and (2). This way, we generate the predicted output sequence $\{\hat{\mathbf{y}}_2(k)\}$. The quality of the identified model is assessed by comparing the predicted output sequence with the measured one. This quality is expressed using the Variance Accounted For VAF [18]:

$$\text{VAF} = \max\left\{0, \left(1 - \frac{\text{var}(\mathbf{y}_2 - \hat{\mathbf{y}}_2)}{\text{var}(\mathbf{y}_2)}\right) \times 100\%\right\}. \tag{6}$$

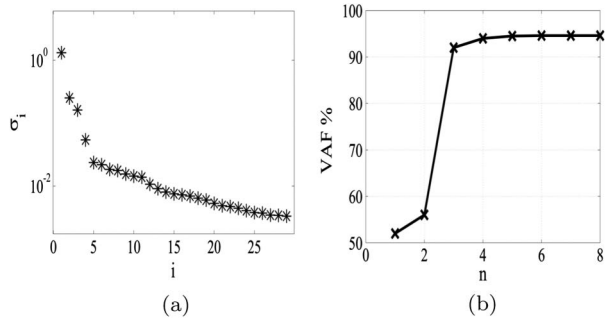


Fig. 4. (a) Singular values of the data matrix used in the identification. (b) The VAF values for different order n of the state-space model (1,2).

If VAF is equal to 100% it means a perfect match between the output that is predicted by the model and the TADM's actual response.

As a first validation, we identified the state-space model when only the central actuator 3 is active (Fig. 1). The input used for identification and the corresponding output are given in Fig. 5(a). The order of the state-space model (1) and (2) is estimated from the singular values and VAF plots given in Fig. 4. By identifying the gaps between the singular values that are shown in Fig. 4(a), we concluded that a relatively good state order estimate is $n = 4$ [18]. Figure 4(b) also confirms this conclusion, where we see that the value of the VAF for $n = 4$ is 93%. On the basis of the identified state-space model, we calculated the transfer function [11] from v_3 to α_3. Figure 5(b) shows a Bode plot [11] of this transfer function. In Figs. 5(c) and 5(d), we compared the TADM's dynamical response and the output of the identified state-space model. As it can be seen from these figures, the identified model of

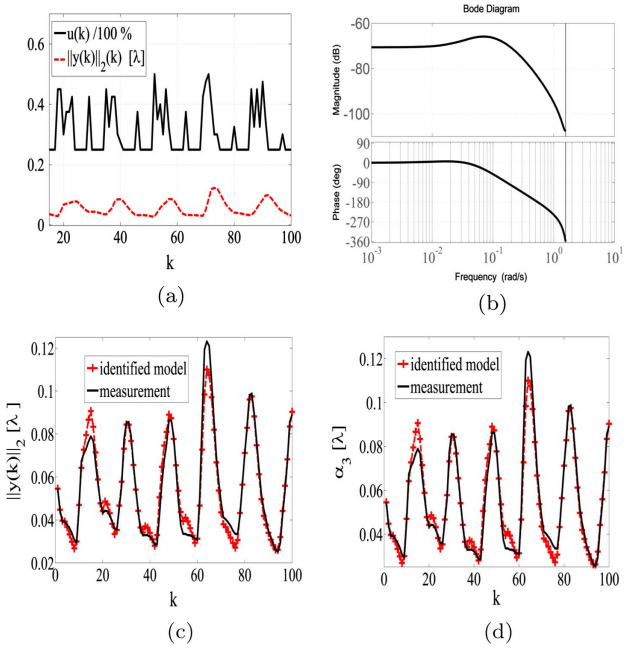


Fig. 5. Identification results when only actuator 3 is active: (a) the input used for identification and the rms of the output. (b) Bode plot of the transfer function between v_3 and α_3. (c) and (d) Prediction and measurements of Zernike coefficients.

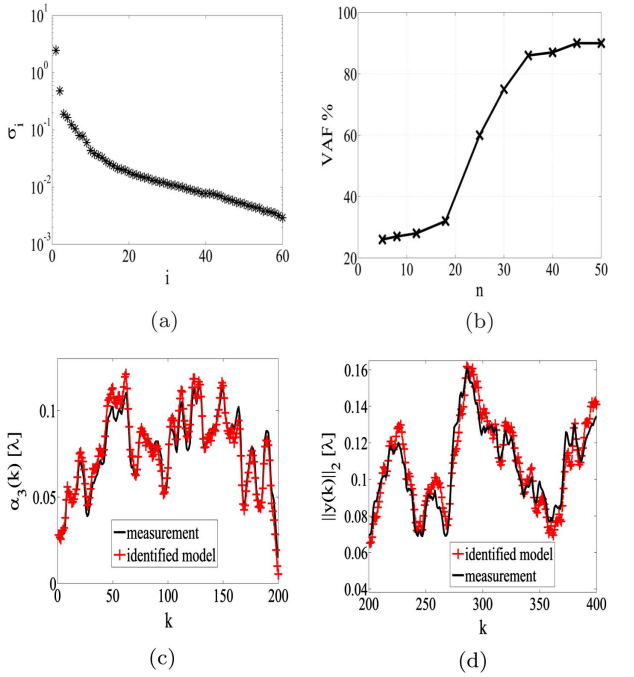


Fig. 6. Identification results when all 19 actuators are active: (a) singular values of the data matrix used for identification; (b) VAF for different model orders n; (c) and (d) prediction performance of the identified model.

the 4th order is able to predict the behavior of the DM with a relatively good accuracy.

Next, we identified the state-space model when all 19 actuators are active (the inputs used for identification were similar to the one that shown in Fig. 5(a)). The order selection is performed on the basis of the singular values and VAF plots shown in Figs. 6(a) and 6(b). From these figures we concluded that a relatively good state order estimate is $n = 40$. The value of VAF corresponding to this state order estimate is roughly 90%. The prediction performance of the identified state-space model (for $n = 40$) is illustrated in Figs. 6(c) and 6(d). As can be observed from these figures, the state-space model (1) and (2) of the 40th order can predict relatively well the TADM's dynamic response.

In conclusion, we have used the subspace identification technique to identify a low-order dynamical model of a TADM prototype. We have demonstrated that the identified state-space model of the 40th order can accurately describe the dynamical behavior of the mirror (90% match). This contrasts to other modeling approaches where the dynamics of the TADM are described by infinite-dimensional system of partial differential equations. Furthermore, the order of the identified model can be additionally decreased using model reduction techniques [10]. The proposed identification procedure is general and can be used to identify dynamical models of other types of TADMs (for example, the types of TADMs proposed in [4,6,7]). Due to its low-dimensionality, the identified model can be used to develop efficient and simple model-based controllers. We are currently working on the implementation of the presented model in an AO system for predictive control of thermally induced aberrations in lithographic systems.

This research is supported by the Dutch Ministry of the Economic Affairs and the Provinces of Noord-Brabant and Limburg in the frame of the Pieken in de Delta program. The authors are grateful to S. F. Pereira and J. A. Meisner for helpful discussions. The authors also wish to thank R. Horsten and R. Pols for technical support.

References

1. O. Albert, L. Sherman, G. Mourou, T. B. Norris, and G. Vdovin, Opt. Lett. **25**, 52 (2000).
2. S. Piehler, B. Weichelt, A. Voss, M. Abdou Ahmed, and T. Graf, Opt. Lett. **37**, 5033 (2012).
3. S. K. Ravensbergen, "Adaptive optics for extreme ultraviolet lithography: actuator design and validation for deformable mirror concepts," Ph.D. thesis (Technische Universiteit Eindhoven, 2012).
4. M. Kasprzack, B. Canuel, F. Cavalier, R. Day, E. Genin, J. Marque, D. Sentenac, and G. Vajente, Appl. Opt. **52**, 2909 (2013).
5. R. Lawrence, D. Ottaway, M. Zucker, and P. Fritschel, Opt. Lett. **29**, 2635 (2004).
6. B. Canuel, R. Day, E. Genin, P. La Penna, and J. Marque, Class. Quantum Grav. **29**, 085012 (2012).
7. G. Vdovin and M. Loktev, Opt. Lett. **27**, 677 (2002).
8. S. K. Ravensbergen, P.C.J. N. Rosielle, and M. Steinbuch, Precis. Eng. **37**, 353 (2013).
9. S. E. Winters, J. H. Chung, and S. A. Velinsky, Mech. Based Des. Struc. Mach. **32**, 195 (2004).
10. A. Chiuso, R. Muradore, and E. Marchetti, IEEE Trans. Control Syst. Technol. **18**, 705 (2010).
11. K. J. Astrom and R. M. Murray, *Feedback Systems: An Introduction for Scientists and Engineers* (Princeton University, 2009).
12. H. Song, R. Fraanje, G. Schitter, G. Vdovin, and M. Verhaegen, Eur. J. Control **17**, 290 (2011).
13. A. Polo, A. Haber, S. F. Pereira, M. Verhaegen, and H. P. Urbach, Opt. Express **20**, 27922 (2012).
14. A. Haber, A. Polo, C. S. Smith, S. F. Pereira, H. P. Urbach, and M. Verhaegen, Appl. Opt. **52**, 2363 (2013).
15. W. Nowacki, *Dynamic Problems of Thermoelasticity* (Springer, 1975).
16. S. Timoshenko and S. Woinowsky-Krieger, *Theory of Plates and Shells* (McGraw-Hill, 1959).
17. M. Laslandes, E. Hugot, and M. Ferrari, J. Eur. Opt. Soc. Rapid Pub. **7**, 12036 (2012).
18. M. Verhaegen and V. Verdult, *Filtering and System Identification: A Least Squares Approach* (Cambridge University, 2007).
19. A. Chiuso, Automatica **43**(6), 1034 (2007).
20. D. Malacara, *Optical Shop Testing* (Wiley-Interscience, 2007).